

Auxin, actin and growth of the *Arabidopsis thaliana* primary root

Abidur Rahman^{1,2}, Alex Bannigan¹, Waheeda Sulaman¹, Priit Pechter³, Elison B. Blancaflor³ and Tobias I. Baskin^{1,*}

¹Biology Department, University of Massachusetts, Amherst, MA 01003, USA,

²Cryobiosystem Research Center, Faculty of Agriculture, Iwate University, Morioka 020-8550, Japan, and

³Plant Biology Division, Samuel Roberts Noble Foundation, Ardmore, OK 73401, USA

Received 25 October 2006; revised 10 January 2007; accepted 12 January 2007.

*For correspondence (fax +1 413 545 3243; e-mail baskin@bio.umass.edu).

Summary

To understand how auxin regulates root growth, we quantified cell division and elemental elongation, and examined actin organization in the primary root of *Arabidopsis thaliana*. In treatments for 48 h that inhibited root elongation rate by 50%, we find that auxins and auxin-transport inhibitors can be divided into two classes based on their effects on cell division, elongation and actin organization. Indole acetic acid (IAA), 1-naphthalene acetic acid (NAA) and tri-iodobenzoic acid (TIBA) inhibit root growth primarily through reducing the length of the growth zone rather than the maximal rate of elemental elongation and they do not reduce cell production rate. These three compounds have little effect on the extent of filamentous actin, as imaged in living cells or by chemical fixation and immuno-cytochemistry, but tend to increase actin bundling. In contrast, 2,4-dichlorophenoxy-acetic acid (2,4-D) and naphthylphthalamic acid (NPA) inhibit root growth primarily by reducing cell production rate. These compounds remove actin and slow down cytoplasmic streaming, but do not lead to mislocalization of the auxin-efflux proteins, PIN1 or PIN2. The effects of 2,4-D and NPA were mimicked by the actin inhibitor, latrunculin B. The effects of these compounds on actin were also elicited by a 2 h treatment at higher concentration but were not seen in two mutants, *eir1-1* and *aux1-7*, with deficient auxin transport. Our results show that IAA regulates the size of the root elongation zone whereas 2,4-D affects cell production and actin-dependent processes; and, further, that elemental elongation and localization of PINs are appreciably independent of actin.

Keywords: cell division, cytoplasmic streaming, elemental elongation, PIN1, PIN2.

Introduction

Growth is the target of the first hormone discovered in plants – a compound named auxin from the Greek *auxein*, meaning to grow. Today, auxin is perhaps the best understood of the plant hormones and the one most resembling the canonical concept of a messenger, synthesized in one place and acting at another. Recently, molecular studies have advanced our understanding of auxin perception and its regulation of gene expression (Badescu and Napier, 2006; Woodward and Bartel, 2005). However, the pace has been slower for understanding the steps after transcription that engage the machinery of growth.

Although it promotes shoot growth, auxin inhibits root growth. Many studies on auxin, both physiological and genetic, report root length. Although easy to assay, root length as a parameter hides considerable complexity

because the length of the root is specified by both cell expansion and division (Beemster and Baskin, 1998; Green, 1976). Furthermore, within an organ growth zone, division and expansion depend not only on the rate at which each process happens in each cell, but also on the numbers of cells dividing and elongating at any one moment. Although auxin has been known for the better part of a century to inhibit root growth, we are generally unaware of the contributions from division and elongation, let alone able to connect the hormone to specific, regulatory steps, such as controlling the length of the elongation zone.

Whereas growth was the original auxin target, an emerging one is the actin cytoskeleton. Many years ago, indole acetic acid (IAA) was reported to stimulate cytoplasmic streaming (Sweeney and Thimann, 1938), a process that

depends on actin. More recently, auxin responses have been found to be defective in transgenic plants expressing dominant-negative or constitutively active Rop GTPases (Yang, 2002), proteins that have been implicated as upstream regulators of actin polymerization (Xu and Scheres, 2005a). Auxin has been argued to promote elongation of rice coleoptiles by reorganizing filamentous actin from coarse bundles to fine strands (Holweg *et al.*, 2004; Wang and Nick, 1998). Furthermore, expression of an actin isoform in Arabidopsis, *ACT7*, is auxin-sensitive, so much so that callus formation is impaired when expression of the isoform is reduced (Kandasamy *et al.*, 2001). Finally, it has been hypothesized that the asymmetric localization of carriers required for the polar transport of auxin is based on dynamic vesicle traffic guided by actin filaments (Blakeslee *et al.*, 2005; Muday and Murphy, 2002).

Although the best understood roles for actin are in organelle motility and cytokinesis (Sano *et al.*, 2005; Smith, 1999; Williamson, 1993), actin also appears to play a direct role in growth. In pollen tubes, growth can be stopped at lower concentrations of actin inhibitors than stop streaming (Vidali *et al.*, 2001), and growth is correlated with the presence in the tip of a complex, actin-rich structure, the cortical fringe (Lovy-Wheeler *et al.*, 2005). These findings imply that actin supports tip growth with more than tracks for vesicle delivery. Trichomes and pavement cells of leaf epidermis require the actin cytoskeleton to generate their complex shapes, probably via mechanisms in addition to targeted secretion (Smith and Oppenheimer, 2005). Finally, widespread growth alterations have been reported following interference with actin function (e.g. Ketelaar *et al.*, 2004).

Therefore, actin has been demonstrated to be important for growth and auxin responses; nevertheless, few of these observations have dealt with specific growth components, and, for the most part, the mechanistic basis for these effects remains obscure. To elucidate the role of actin in growth and auxin responsiveness, we chose to study primary root growth in Arabidopsis. In roots, elemental elongation rate is an order of magnitude faster than in stems or leaves, and the Arabidopsis root is thin and lacks chlorophyll, making it ideal for imaging.

The objective of the work reported here was to determine which growth components are affected by auxin, and to what extent these auxin responses are mediated by actin. In our experiments, seedlings were treated with concentrations of auxins, or other compounds, that reduce root elongation rate by approximately 50% and assayed after 48 h. In this way, steady-state responses are attained and treatments are comparable; also, the likelihood of non-specific effects is minimized, and the auxin treatments may resemble a developmental modification of root growth rather than its termination. To delineate growth components, we characterized root growth kinematically. To assess

actin, we used imaging of living cells as well as chemical fixation followed by antibody staining.

Results

Comparison of elongation and cell division in response to auxins

The native auxin, indole acetic acid (IAA), is susceptible to photolysis from blue and ultraviolet light; therefore, all experiments reported here used plants grown in yellow light, which prolongs the lifetime of IAA in growth media (Stasinopoulos and Hangarter, 1990). To characterize the mechanism of inhibition of root elongation by auxin, we pursued a kinematic approach. First, we evaluated the time course of root elongation rate (Figure 1a–c). Seedlings were grown for 4 days, transplanted onto medium with auxins as indicated, and root elongation rate measured each day for 3 days. The elongation rate of control roots increased each day, an acceleration caused almost exclusively by increasing cell production (Beemster and Baskin, 1998). The synthetic auxin, 2,4-dichlorophenoxy-acetic acid (2,4-D), led to a steady-state root elongation rate over the 3 days at 30 nM, whereas none of the tested concentrations of IAA or of another synthetic auxin, 1-naphthalene acetic acid (NAA), produced steady-state kinetics. On day 3, the sensitivity of root elongation to IAA and 2,4-D was essentially equal, whereas the sensitivity to NAA was lower (Figure 1d). For further work, we used 30 nM IAA, 30 nM 2,4-D and 100 nM NAA, these being the concentrations that reduce elongation rate by about 50%, and (except where noted) examined their effects after 2 days of treatment.

To evaluate the impact of auxin on cell division and elongation, we measured root elongation rate and the length of newly mature cortical cells. The ratio of mature cell length to elongation rate gives the time required to produce one cortical cell (per cell file); the inverse of this time gives the rate at which the file produces cells (Silk *et al.*, 1989). This rate of cell production represents the output of the meristem (for that file of cortical cells), reflecting both the number of dividing cells and their rates of division. All the auxins reduced cell length significantly, suggesting that they reduced cellular elongation (Table 1). IAA and NAA reduced cell length proportionally to their reduction of elongation rate, indicating that these auxins did not affect cell production rate. In contrast, 2,4-D reduced cell length to a lesser extent than its effect on elongation rate and thus reduced cell production rate substantially.

The effect of these auxins on cell division was also investigated by means of expression of a cell-cycle reporter, *Cyc1B*;1-GUS, constructed so that the glucuronidase is present chiefly during M phase (Colón-Carmona *et al.*, 1999). Preliminary experiments showed that the line harboring this construct responded to the auxins indistinguish-

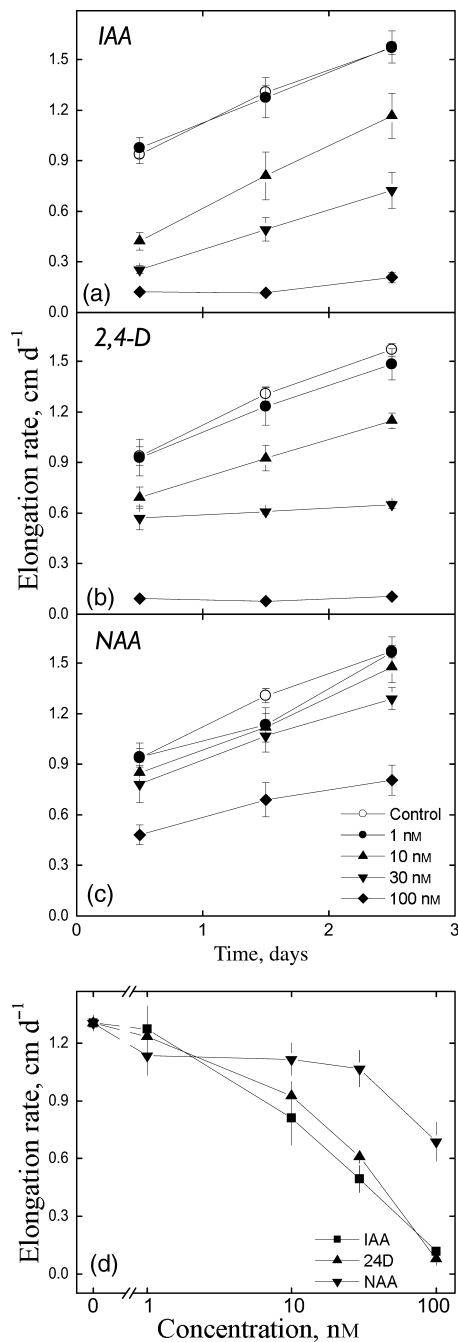


Figure 1. Effect of auxins on Arabidopsis primary root elongation. (a–c) Time courses. (d) Dose–response curves for the third day of treatment. Symbols show the means \pm SEM for three replicate experiments. Four-day-old seedlings were transplanted onto treatment plates at time 0.

ably from the wild type (data not shown). The pattern of GUS expression in seedlings treated with 30 nM IAA appeared identical to that in controls, whereas fewer cells were stained in seedlings treated with 30 nM 2,4-D (Figure 2). Counts of blue-stained cells gave a significant difference from the

control only for the 2,4-D treatment (not shown). The kinematic data (Table 1) and the GUS staining concur in showing that 2,4-D targets cell division whereas IAA and NAA do not.

Because the relationship between mature cell length and elongation is indirect, we quantified elongation spatially, taking advantage of software, RootflowRT, developed for this purpose (van der Weele *et al.*, 2003). RootflowRT quantifies the spatial profile of velocity, specifically calculating the component of velocity parallel to the midline of the root (or when the root is bent, parallel to the local tangent of the midline). The derivative of the velocity profile is the profile of elemental elongation rate (Silk, 1992). The elemental elongation rate characterizes the deformation of subcellular (i.e. elemental) regions of cell wall and therefore is close to the physical processes of expansion.

In a root, the velocity profile can be divided into three regions: a region where velocity increases gradually with position, corresponding approximately to the meristem; a region where velocity increases steeply with position, corresponding to the elongation zone; and a region where velocity becomes constant, at a value that equals the rate of root elongation, corresponding to the mature zone (Figure 3). The three regions are separated by two transitions, with the transition between meristem and elongation zone generally being more abrupt than the one between the elongation and mature zone. To compare profiles among roots and treatments, we fitted a function to the data (Figure 3, thin red line). Parameters of the fitted function include the x-axis coordinates of the midpoints for the two transitions, and a value that measures their abruptness. Additionally, the spatial derivative of the fitted function yields the profile of elemental elongation rate. The function has been described fully elsewhere (Peters and Baskin, 2006).

The velocity profiles for the auxins resembled that of the control, except, as expected, the final velocity was reduced by about one-half. Along with reduced velocity, all of the auxins reduced the length of the growth zone by roughly 50% (Table 2). Neither IAA nor 2,4-D reduced the maximal rate of elemental elongation, while NAA reduced the rate by 25% (Figure 3, thick blue lines, and Table 2).

Almost always, the length of the elongation zone and the rate of cell production are well correlated (Beemster and Baskin, 1998; Beemster *et al.*, 2002); it is therefore unusual that IAA cut in half the length of the elongation zone without reducing cell production rate. A possibility is that IAA shrank the length of cells leaving the meristem by 50%; but, as seen below, such a reduction was not apparent. Because the zone of elongation in an IAA-treated root was shortened but cell production and maximal elemental elongation rate were undiminished, cells resided within that zone for less time than in controls; a decrease in residence time also occurred for NAA- and 2,4-D-treated

Table 1 Effect of auxins on cell length and cell production in the Arabidopsis primary root

| Treatment | Elongation rate (mm day ⁻¹) | Cell length (μm) | Cell production rate (cells day ⁻¹) |
|-------------|---|------------------|---|
| Control | 9.19 ± 0.15 (100) | 180 ± 4.2 (100) | 50.7 ± 1.4 (100) |
| 30 nM IAA | 3.67 ± 0.10 (40) | 71 ± 2.2 (40) | 51.9 ± 0.5 (102) |
| 100 nM NAA | 5.69 ± 0.10 (62) | 113 ± 1.4 (62) | 50.6 ± 0.7 (100) |
| 30 nM 2,4-D | 4.10 ± 0.30 (44) | 137 ± 4.6 (76) | 33.5 ± 1.5 (66) |

Data are means ± SEM of three replicate experiments. Values in parentheses are the percentage of control for each column. Seedlings were exposed to the treatments for 3 days and the measurements reflect the behavior over the third day of treatment.

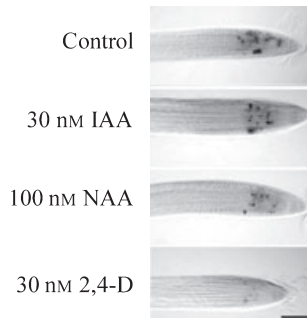


Figure 2. Effect of auxins on expression of a reporter for M-phase, CycB1;1-Gus, in the primary root tip. Images are representative of 7–10 roots treated as for Figure 1 and examined on the third day of treatment. Bar = 100 μm.

roots, although the decrease is smaller than for IAA treatment because the decrease in cell production rate on 2,4-D, and in elemental elongation rate on NAA, tend to increase residence time. The time spent by a cell in the elongation zone might be regulated specifically by auxin. In support of this, the transition to zero growth at the base of the elongation zone tended to be sharper in IAA-treated roots compared with that of controls (Table 2). Alternatively, auxin could regulate the position where elongation ends. The concept of auxin controlling the *length* of the elongation zone, whether through spatial or temporal

means, contrasts the usual view of auxin as inhibiting (in roots) the mechanism of expansion.

Effect of auxin on the actin cytoskeleton

To understand the underlying mechanism of auxin-induced inhibition of growth and division, we investigated actin organization. Seedlings were treated to inhibit root elongation by approximately 50% and actin imaged after 2 days, the same conditions as used for the analyses of growth reported above. First, we imaged actin by chemical fixation followed by staining with an anti-actin antibody. IAA and NAA tended to increase the intensity of fluorescence, in both meristem and elongation zone (Figure 4a–f); however, this response was subtle. In contrast, 2,4-D led to the widespread loss of detectable filaments (Figure 4g,h). This was accompanied by increased non-filamentous background, present throughout the cell in the meristem and often concentrated at end walls in the elongation zone.

To confirm these results, we imaged actin in living cells, by means of a transgenic line expressing a GFP-tagged actin-binding domain from fimbrin (ABD2-GFP) (Wang *et al.*, 2004). Preliminary experiments showed that this line responded to the auxins with reductions in root elongation rate equivalent to those of the wild type. On IAA or NAA, fluorescence from the reporter tended to increase, and the filaments often appeared to be thicker and more bundled (Figure 5a–f), but, as with chemical fixation, this increase

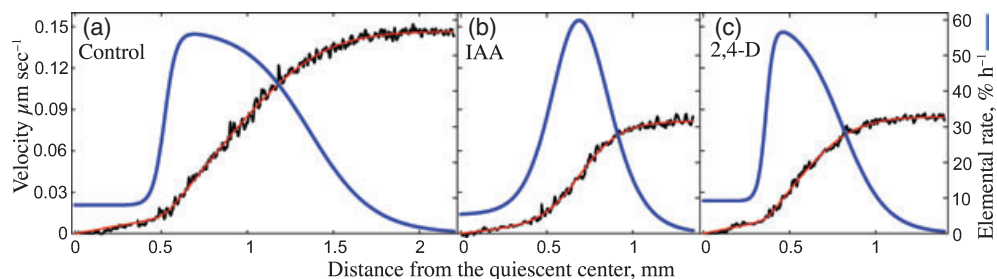


Figure 3. High-resolution analysis of elongation in Arabidopsis roots exposed to auxins.

(a) Control. (b) 30 nM IAA. (c) 30 nM 2,4-D. Velocity profiles (jagged black line) were obtained with RootflowRT and fitted with a modified logistic function (thin red line). The fitted function was differentiated to give the elemental elongation rate (thick blue line, right-hand y axis). Treatments were as for Figure 1 and roots were examined after 48 h. Data are for single representative roots.

Table 2 Effects of auxins on selected root growth parameters obtained from high-resolution spatial analysis of growth

| Treatment | Final velocity ($\mu\text{m sec}^{-1}$) | Growth zone length (mm) | Maximal elemental elongation rate ($\% \text{h}^{-1}$) | Transition ratio |
|--------------------------|---|-------------------------|--|------------------|
| Control | 0.147 ± 0.019 (100) | 1.87 ± 0.24 (100) | 55 ± 5.7 (100) | 3.1 ± 1.6 |
| 30 nM IAA | 0.078 ± 0.014 (54) | 1.01 ± 0.12 (54) | 56 ± 7.1 (101) | 1.3 ± 0.9 |
| 100 nM NAA | 0.062 ± 0.009 (42) | 0.99 ± 0.09 (53) | 42 ± 4.0 (77) | 1.2 ± 1.0 |
| Control ^a | 0.129 ± 0.024 (100) | 1.92 ± 0.12 (100) | 47 ± 7.0 (100) | 4.1 ± 2 |
| 30 nM 2,4-D ^a | 0.07 ± 0.014 (54) | 1.09 ± 0.15 (57) | 46 ± 5.9 (99) | 3.7 ± 2 |

^aThese treatments represent a separate group of experiments.

Roots imaged after 48 h of treatment. Data are means \pm SD for 6–12 roots, imaged from at least three different experiments. Values in parentheses are the percentage of control. Parameters were obtained from the customized logistic function fitted to the data as follows: ‘final velocity’ is the position where the fitted curve reached 95% of the asymptote (and estimates overall root elongation rate), ‘growth zone length’ is the value of the second transition (from elongation to mature zones), ‘maximal elemental elongation rate’ is the maximum of the derivative of the fitted function, and ‘transition ratio’ is the ratio of the parameters characterizing the abruptness of the transitions, with values greater than 1 indicating that the first transition is more abrupt than the second.

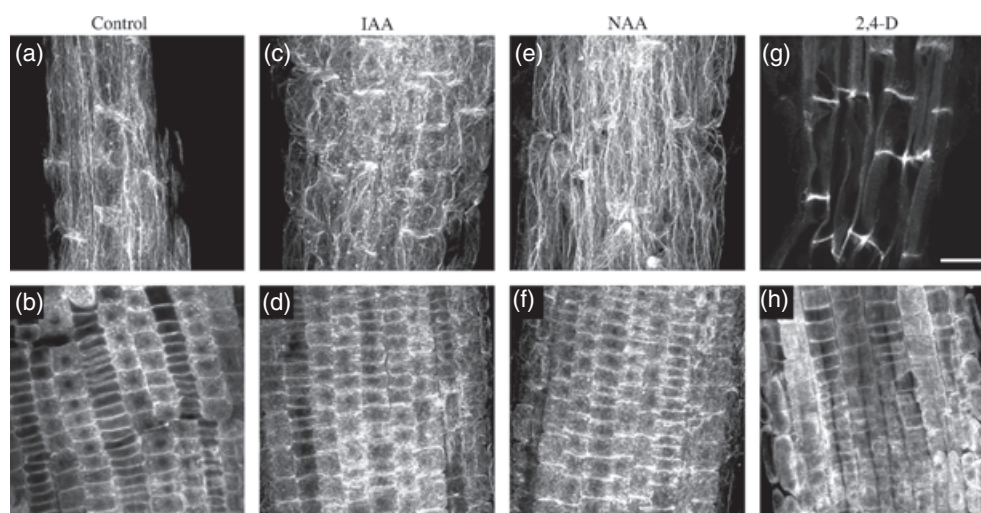


Figure 4. Effects of auxins on filamentous actin: chemical fixation.

(a, b) Control. (c, d) 30 nM IAA. (e, f) 100 nM NAA. (g, h) 30 nM 2,4-D. The top row shows the elongation zone, the bottom row shows the meristem. The images are representative of at least three fixation runs, with 3–5 roots per treatment in each run. Roots were fixed after 2 days of treatment and actin was localized using immuno-cytochemistry and imaged using confocal fluorescence microscopy. Images are projections of 10–12 optical sections. Bar = 25 μm .

was subtle. On 2,4-D, although some actin filaments remained, their extent was reduced, and the remnant filaments often appeared to emanate from a central focus not typical of controls (Figure 5g,h). Furthermore, cells in 2,4-D-treated roots, but not those in other treatments, contained bright, punctate structures. Images from both methods indicate that 2,4-D disrupts the actin cytoskeleton.

Effects of latrunculin B on root growth and actin organization

The unexpected finding that 2,4-D disrupted the actin cytoskeleton led us to compare the 2,4-D effect with that of a bona fide actin inhibitor, latrunculin B. To enable meaningful comparison with the auxins, we first determined that root elongation was reduced by about 50% on 17 nM latrunculin

on the third day of treatment (Figure 6a). This concentration was sufficient to remove a considerable amount of actin (Figure 6e,f). In some cells, radial foci of actin filaments appeared (Figure 6e), whereas in others there was a more general loss of polymerized actin (Figure 6f). These effects of latrunculin resemble those of 2,4-D, except that latrunculin rarely generated puncta.

We next assessed the effects of 17 nM latrunculin on elongation and division. Latrunculin reduced cell production rate strongly and maximal elongation modestly (Figure 6b,c and Table 3). Note that, in these experiments, the average reduction in root elongation rate was 70%, a greater level of inhibition than the 50% obtained above for the auxins. Overall, latrunculin affected elongation and division similarly to 2,4-D, which suggests that the disruption of actin caused by 2,4-D is sufficient to account for its effect on cell production and hence on root growth.

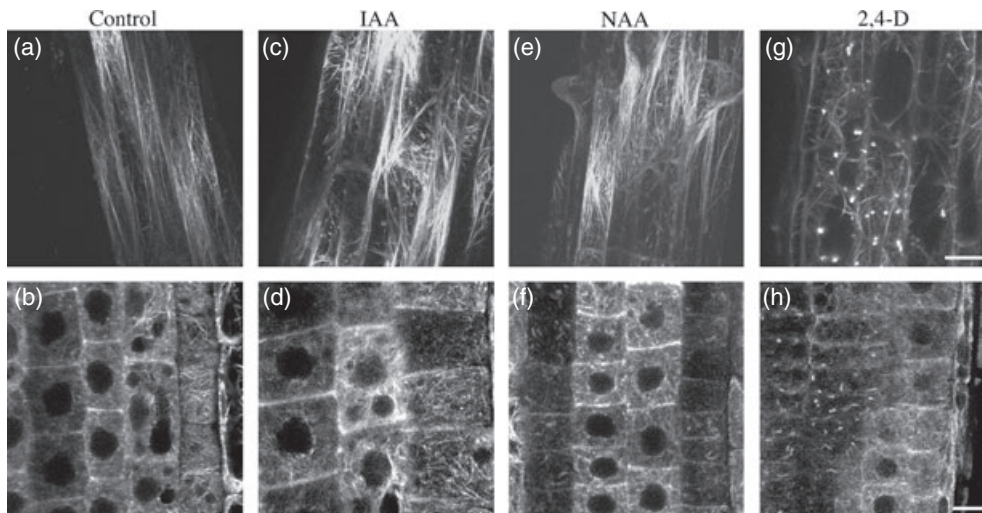


Figure 5. Effects of auxins on filamentous actin: ABD-GFP expression. (a, b) Control. (c, d) 30 nM IAA. (e, f) 100 nM NAA. (g, h) 30 nM 2,4-D. The top row shows the elongation zone, the bottom row shows the meristem. The images are representative of 3–6 separate imaging runs, with 4–6 roots per treatment in each run. Roots were imaged after 48 h of treatment. Images are projections of 10–12 optical sections. Bar in (g) = 25 μm and relates to (a, c, e, g); bar in (h) = 10 μm and relates to (b, d, f, h).

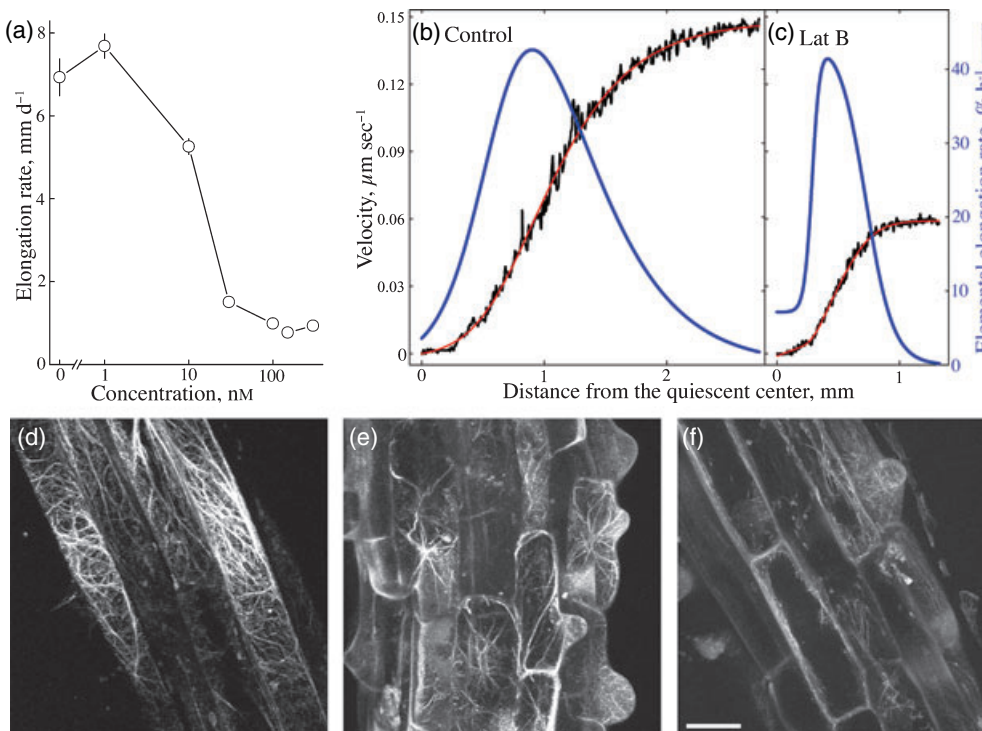


Figure 6. Effects of an actin inhibitor, latrunculin B, on root elongation and actin appearance. (a) Root elongation rate as a function of latrunculin concentration. Two-day-old seedlings were transplanted on to drug plates and measured on the third day of treatment. Data are means \pm SEM of three replicate plates. Control rates are lower than in Figure 1 because younger plants were used on smaller plates to conserve the inhibitor. The half-maximal inhibition of elongation was at about 17 nM. (b, c) Spatial analysis of elemental elongation, as for Figure 3. (d–f) Actin filaments imaged with ABD-GFP. (d) Control. (e, f) Treatment with 17 nM latrunculin after 48 h. Representative images from four separate imaging runs, with at least three roots per treatment in each run. Images are projections of 10–12 optical sections. Scale bar = 25 μm .

Table 3 Effects of latrunculin on selected growth parameters

| Treatment | Root growth rate (mm day ⁻¹) | Cell length (μm) | Cell production rate (cell day ⁻¹) | Maximum elemental rate ^a (% h ⁻¹) |
|---------------------|--|------------------|--|--|
| Control | 7.5 ± 0.17 | 162 ± 4 | 46.5 ± 0.5 | 46 ± 6 |
| 17 nM latrunculin B | 3.4 ± 0.14 (45) | 105 ± 11 (65) | 33.2 ± 3.6 (71) | 35 ± 7 (76) |

Data are means ± SEM of three replicate plates. Values in parentheses are the percentage of control. Seedlings were exposed to the treatments for 3 days, and the measurements reflect the behavior over the third day of treatment.

^aThese data were obtained from separate experiments for spatial analysis. Data are means ± SD for five (control) and nine (latrunculin B) roots.

Actin and auxin transport

Because distinct effects of IAA and 2,4-D are often interpreted in terms of polar auxin transport, we investigated to what extent altering auxin transport affected actin structure. For this, we first used two polar transport inhibitors, naphthylphthalamic acid (NPA) and tri-iodobenzoic acid (TIBA) (Rubery, 1987). Preliminary dose–response assays found that the root elongation rate was inhibited by 50% at 10 μM NPA and 40 μM TIBA. At these concentrations, roots meandered on the surface of the vertical plate, an impairment in gravitropism implying that polar transport had indeed been reduced.

At these concentrations, NPA and TIBA had contrasting effects on actin organization. NPA reduced filamentous actin and generated puncta (Figure 7b), resembling the effects of 2,4-D. On the other hand, TIBA tended to increase fluorescence intensity and to cause bundling (Figure 7c), similar to the changes induced by IAA and NAA. Diminished actin on treatment with NPA but not TIBA was confirmed with chemical fixation (data not shown). Insofar as TIBA often acts like a weak auxin, the similarity of TIBA and IAA treatment is understandable; the distinction between TIBA and NPA (Figure 7a–c) indicates that the disruptive effect of 2,4-D on actin is unlikely to be explained by an inhibition of polar auxin transport.

To examine further the consequences of altered auxin transport on actin organization, we imaged actin in two mutants with impeded polar transport: *eir1-1*, which reduces auxin efflux, and *aux1-7*, which reduces influx (Luschign *et al.*, 1998; Rahman *et al.*, 2001; Rashotte *et al.*, 2003). We crossed the ABD2–GFP line into each mutant and examined actin by confocal microscopy in F₃ plants expressing the mutant phenotype and ABD2–GFP. The actin cytoskeleton in *aux1-7* was indistinguishable from that of controls, whereas actin in *eir1-1* tended to be modestly bundled and brighter (Figure 7d–f), similar to the actin phenotype observed for IAA, NAA and TIBA treatments. Taken together, these results suggest that the disruption of actin caused by NPA and 2,4-D is not a consequence of inhibited polar auxin transport.

To assess further the link between actin organization, cell division and elongation, we assayed cell production rate in the presence of NPA and TIBA. Consistent with the results

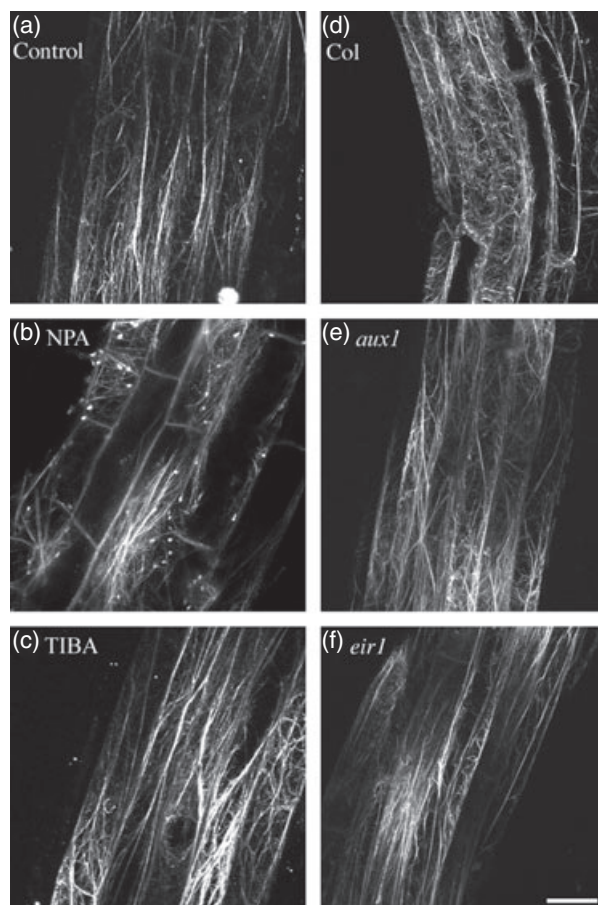


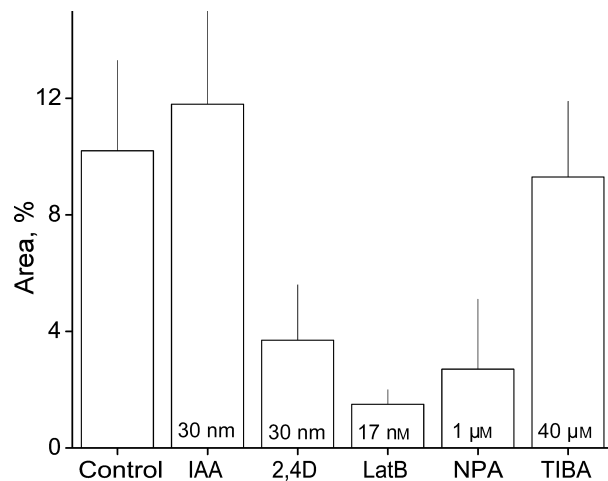
Figure 7. Effect of auxin-transport inhibitors on actin appearance. (a) Control. (b) 10 μM NPA. (c) 40 μM TIBA. (d) Columbia. (e) *aux1-7*. (f) *eir1-1*. (a–c) Treatment for 48 h. The results show ABD2–GFP expression, and are representative images from two (*aux1-7*, *eir1*) to five separate imaging runs, with 4–6 roots per treatment in each run. Images are projections of 10–12 optical sections. Bar = 25 μm.

above, we found that NPA, which disrupts actin, inhibited cell production rate, whereas TIBA reduced cell production rate only modestly (Table 4). These results confirm distinct actions of TIBA and NPA and substantiate the link between disrupted actin and decreased cell production.

Table 4 Effect of auxin-transport inhibitors on root cell length and cell production

| Treatment | Root growth rate (mm day ⁻¹) | Cell length (μm) | Cell production rate (cells day ⁻¹) |
|------------|--|------------------|---|
| Control | 10.1 ± 0.3 (100) | 199 ± 4 (100) | 50.8 ± 1.1 (100) |
| 10 μM NPA | 4.6 ± 0.3 (45) | 143 ± 6 (72) | 32.5 ± 1.5 (64) |
| 40 μM TIBA | 5.6 ± 0.2 (55) | 123 ± 1 (61) | 46.0 ± 1.4 (91) |

Data are means ± SEM of three replicate plates. Values in parentheses are the percentage of control for each column. Seedlings were exposed to the treatments for 3 days and the measurements reflect the behavior over the third day of treatment.

**Figure 8.** Quantification of the extent of actin polymerization.

Bars show the mean and SD of a parameter reflecting the area occupied by actin filaments. Images used were of ABD2-GFP fluorescence from the elongation zone, with treatments as described for Figure 5, upper row, Figure 6e,f and Figure 7b,c. Data are for 10–20 images per treatment, imaged on many different days. The quantification procedure is described in Experimental procedures.

Quantitative assessment of the extent of actin filaments

Because it was surprising that the two auxins and the two auxin-transport inhibitors had such distinct effects on the extent of polymerized actin, we quantified the appearance of actin by using an image-processing method applied previously to microtubules (Tian *et al.*, 2004) and described briefly in Experimental procedures. Images were analyzed representing 10–20 roots for each experimental treatment collected on several days. The extent of polymerised actin was lower specifically in the 2,4-D, latrunculin and NPA treatments (Figure 8), confirming the appearance of the images. This method responds weakly to intensity and so cannot assess the increased fluorescence observed qualitatively in the IAA, NAA and TIBA treatments.

Effect of auxins on cytoplasmic streaming

The degradation of actin observed with 2,4-D or latrunculin treatment was partial; some polymerized actin remained. To

assess the functional significance of this actin, we assayed cytoplasmic streaming, a process known to depend on a functional actomyosin system (Williamson, 1993). During the third day of treatment, the root of intact seedlings was mounted in the same treatment solution, and mature epidermal cells observed with Nomarski optics. Control roots and 30 nM IAA-treated roots streamed vigorously; however, roots treated with either 30 nM 2,4-D or 17 nM latrunculin streamed slowly (Movies S1–S4). These results show that the 2,4-D and latrunculin treatments compromised actin-based motility.

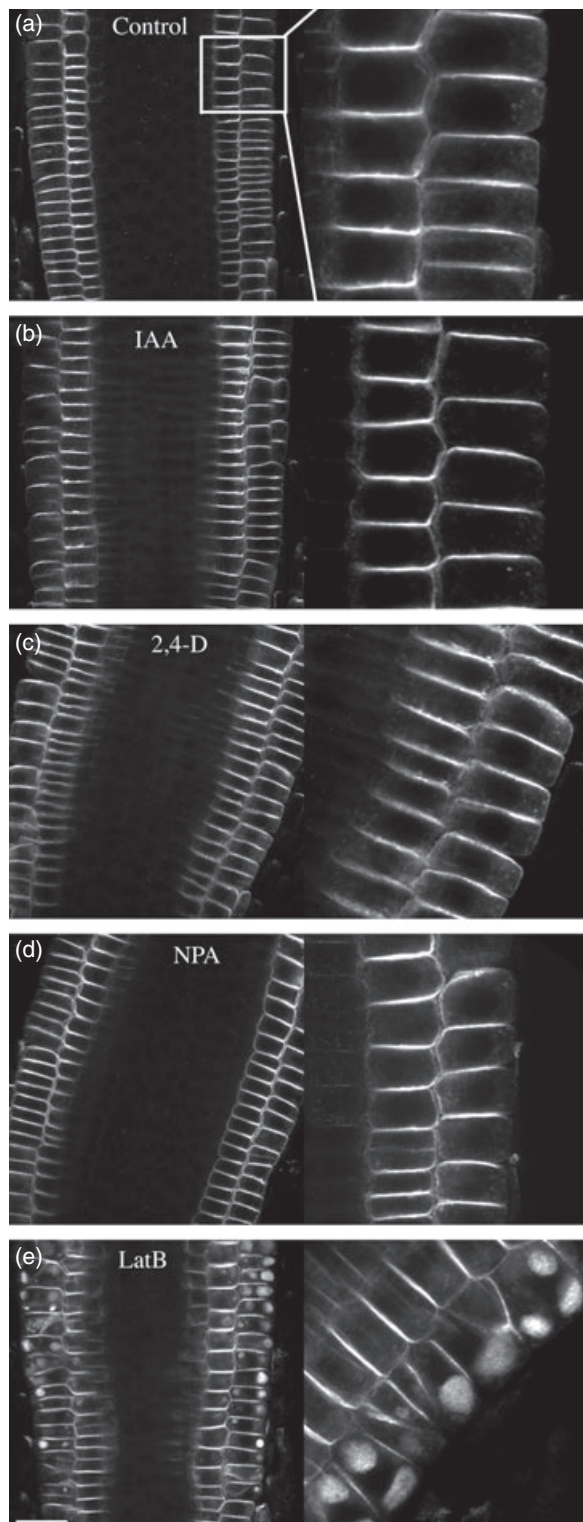
Role of actin in localizing auxin-efflux proteins, PIN1 and PIN2

To assess further consequences of the disruption of actin caused by 2,4-D, we examined PIN auxin-efflux proteins because they are thought to reach their polarized locations in the plasma membrane via actin-dependant trafficking. We first examined the localization of PIN2 using a specific antibody (Boonsirichai *et al.*, 2003). In median, longitudinal optical sections, PIN2 is localized on the shoot-ward side of epidermal cells but on the root-ward side of cortical cells (Figure 9a). We use the terms 'shoot-ward' (for towards the shoot tip) and 'root-ward' (for towards the root tip) because of the conflict in the root between anatomical and developmental referents implied by the terms 'apical' and 'basal'. Despite the two-day treatment, PIN2 localization was not altered visibly with IAA, NAA, 2,4-D, NPA or latrunculin (Figure 9). Latrunculin, but not 2,4-D, led to oblique divisions and large inclusion bodies in epidermal cells; however, these effects were far less prominent when roots were treated with a different actin inhibitor, cytochalasin D (at 8 μM, a concentration that inhibits root growth by 50%; data not shown).

Because most evidence supporting actin-based subcellular localization of PIN proteins has been obtained with PIN1, we also examined this protein. Although PIN1 is reported to be localized correctly in short-term treatments with actin inhibitors (e.g. Geldner *et al.*, 2001), some mislocalization might be expected from the long treatments studied here, involving as they do 30–50 cell divisions per day, per file. Nevertheless, subcellular PIN1 localization appeared unaffected by any of the treatments (Figure S1), implying actin independence for the machinery targeting PIN1 as well as PIN2.

The preceding experimental conditions involved a 2-day treatment; it is therefore possible that correct localization was restored gradually, despite the dismantled actin cytoskeleton. To determine whether short-term disruptions of actin caused mislocalization of PIN2, we examined roots after a 2 h treatment, using a *pin2* mutant line complemented by the expression of a translational PIN2-GFP fusion (Xu and Scheres, 2005b). Fluorescence from PIN2-GFP in the

meristem was bright along the side walls, tending to obscure the polar localization in medial views (data not shown); therefore, we examined epidermal cells in glancing view, in which polar localization was clear. Preliminary experiments showed that the concentrations of growth



regulators used above had little effect on actin in 2 h. Higher concentrations affected actin in 2 h to a similar extent as lower concentrations given over 2 days, except that neither 2,4-D nor NPA caused punctate fluorescence (Figure 10, left-hand panels). In this short-term exposure, disrupted actin in the 2,4-D and NPA treatments was accompanied by apparently unaltered polar localization of PIN2 (Figure 10, right-hand panels). Taken together, the results of the 2-day and 2 h treatments imply that targeting of PIN2 is independent of actin.

Discussion

We report here that three auxins and two auxin-transport inhibitors can be divided into two classes based on their effects on cell division, elongation and the actin cytoskeleton. IAA, NAA and TIBA slow root growth primarily through reducing the extent of the growth zone; these compounds may bundle or increase the fluorescence of filamentous actin. In contrast, 2,4-D and NPA inhibit root growth primarily by reducing cell production rate; these compounds cause depolymerization of actin and slow down cytoplasmic streaming, but do not affect localization of the PIN proteins (Figure 11). Given the central roles of auxin and actin in plant development, it is reasonable to find interactions between them. What appears surprising is that actin provides a basis for separating responses to IAA and 2,4-D, and also that actin function is, at least partially, dispensable for rapid, elemental elongation as well as for PIN targeting.

IAA and 2,4-D evoke differential responses in regulating root growth

When auxins were used at concentrations that inhibited overall root elongation rate by 50%, elemental elongation tended to be unaffected: maximal elemental elongation rate was reduced modestly by NAA and not at all by 2,4-D or IAA (Figure 3 and Table 1). Unaffected elemental elongation contradicts the way auxin is often assumed to act in roots: because auxin promotes growth in stems by loosening the cell wall, it is assumed to inhibit growth in roots by cell-wall tightening (e.g. Liszkay *et al.*, 2004). Tighter cell walls would reduce elemental elongation rates, contrary to our data, and in fact, to previous reports. In *Arabidopsis* exposed to 30 nM 2,4-D from germination onwards, maximal elemental elon-

Figure 9. Effects of auxins and other compounds on the localization of PIN2. (a) Control. (b) 30 nM IAA. (c) 30 nM 2,4-D. (d) 10 μ M NPA. (e) 17 nM latrunculin B. Four-day-old seedlings were treated for 48 h before being fixed and processed for immunofluorescence with an anti-PIN2 antibody. Left-hand panels show survey views and right-hand panels show a higher magnification, as indicated by the box in (a). The images are representative of three or four separate imaging runs, with four to six roots per treatment in each run. Images are single confocal sections. Bar = 25 μ m.

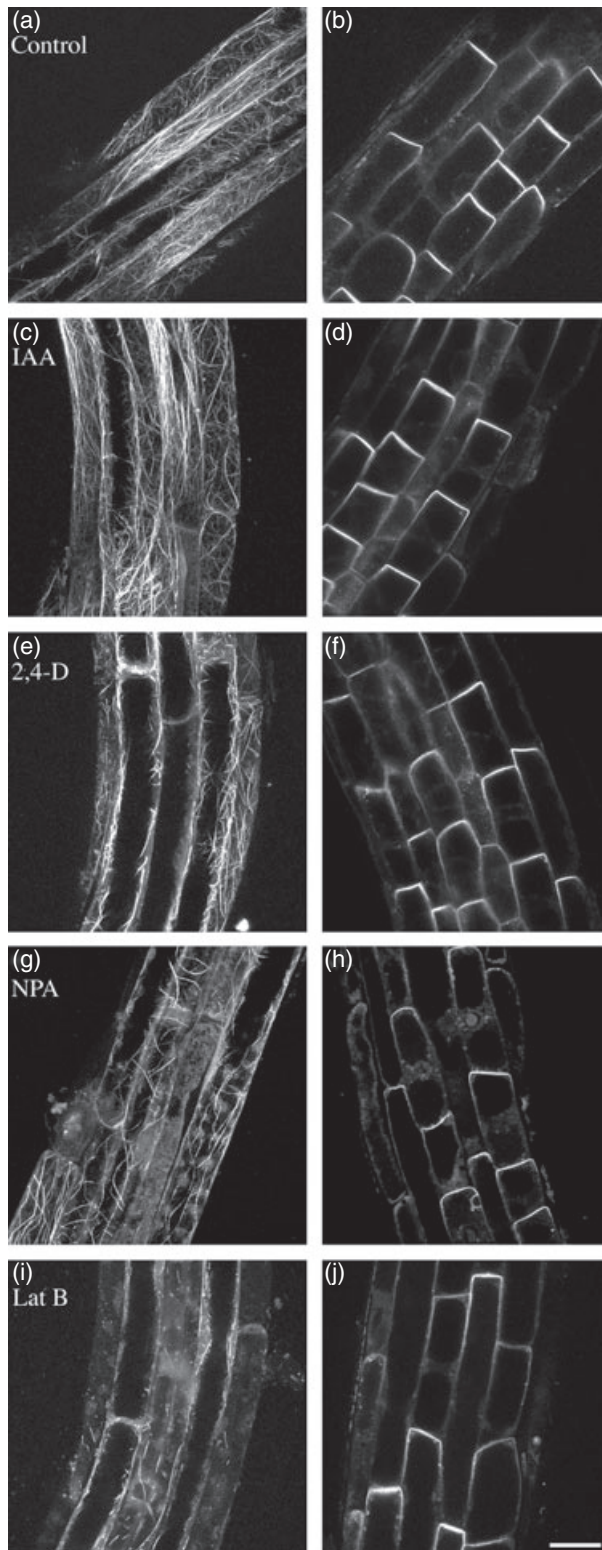


Figure 10. Actin and PIN2 in seedlings treated at high concentration for 2 h. (a, b) Control. (c, d) 1 μM IAA. (e, f) 1 μM 2,4-D. (g, h) 100 μM NPA. (i, j) 1 μM latrunculin B. ABD2-GFP (left-hand panels) and GFP-PIN2 (right-hand panels) in epidermis (root tip is towards the bottom of the page). Images are representative of two imaging runs, with four to six roots per treatment. Bar = 25 μm.

gation rate was the same as in the controls (Beemster and Baskin, 2000). In wheat (*Triticum aestivum*) treated with low and modest concentrations of IAA, the elemental elongation rate was transiently inhibited throughout the elongation zone, and then, after about 1 h, recovered to values the same as or even greater than the control (Hejnowicz, 1961). In timothy (*Phleum pratense*), although high concentrations of IAA reduced elemental elongation, low concentrations caused only transient inhibition, similar to wheat (Goodwin, 1972). In all these reports, whether or not the maximal elemental elongation rate was transiently inhibited, auxins reliably shortened the zone of elongation. In 2,4-D-treated roots, the growth zone is shortened at least in part because cell division rate is decreased, thus decreasing the flux of cells into the elongation zone (Beemster and Baskin, 2000), whereas we found for IAA treatment that the size of the elongation zone itself appears to be regulated. Therefore, in roots, IAA acts over the whole growth zone to restrict its span, rather than acting cell autonomously to limit wall loosening.

In principle, IAA could control the span of the growth zone either by enforcing a boundary where cells stop elongating or by enforcing the duration that a cell spends elongating. When IAA is applied to a limited region of the growth zone of the maize root, the shoot-ward part of the zone responds much less than the root-ward part (Davies *et al.*, 1976; Meuwly and Pilet, 1991), observations that are in accordance with a program of temporal regulation established while cells are in or near the meristem.

The synthetic auxin, 2,4-D, has been used for decades as a chemical analogue of IAA because of its stability and auxin-like action. 2,4-D and IAA are widely assumed to share the same signal-transduction pathways and to differ only in transport or metabolism (e.g. Taiz and Zeiger, 2006). However, distinct signal transduction paths are being uncovered.

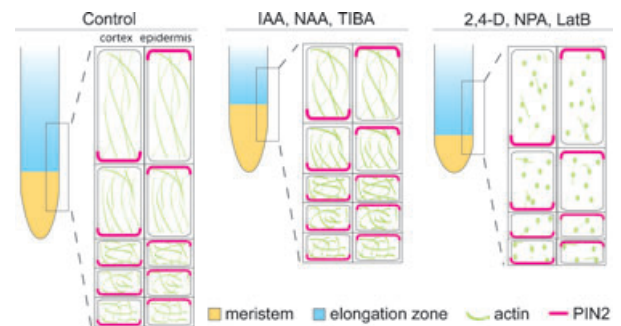


Figure 11. Schematic representation of the key results.

IAA, NAA and TIBA slow root growth primarily by reducing the length of the elongation zone with little or no decrease in cell production. These compounds tend to bundle actin filaments. In contrast, 2,4-D, NPA and latrunculin slow root growth primarily by decreasing the number of dividing cells, although they decrease cell elongation to some extent. These compounds depolymerize actin filaments, but do not affect the subcellular localization of PIN proteins.

In *Arabidopsis*, 2,4-D binds the auxin receptor SCF-TIR1 with notably lower affinity than IAA does (Kepinski and Leyser, 2005); moreover, sensitivity to 2,4-D is conferred by a protein, SMAP1, that does not confer sensitivity to IAA (Rahman *et al.*, 2006). The discovery of SMAP1 supports the idea that native and synthetic auxins are perceived by mechanistically distinct pathways, albeit partially overlapping. If plants perceive auxins distinctly, then it follows that plants may respond to them distinctly.

It has been reported for several years that auxin affects cell division predominantly through a G-protein pathway, while it affects expansion through a pathway involving an auxin receptor, ABP1 (Chen, 2001; Ullah *et al.*, 2003); recently, 2,4-D was shown to activate the division pathway preferentially whereas NAA acted preferentially on expansion (Campanoni and Nick, 2005). This was observed in tobacco tissue culture cells, making an explanation based on differential transport unlikely. Similar to the results on tobacco cells, we show here that 2,4-D mainly affects cell division and IAA affects elongation (Figure 3 and Table 1). Further, these auxins exhibit contrasting effects on the actin cytoskeleton, with 2,4-D disrupting it (Figures 4, 5, 8 and 10). High concentrations of IAA did not remove actin (Figure 10), implying that the difference between 2,4-D and IAA effects cannot be explained by the 2,4-D-treated root having a higher intracellular auxin concentration. Collectively, these results support the idea that 2,4-D and IAA response pathways are mechanistically distinct.

In agriculture, 2,4-D is an important herbicide even though its mechanism of toxicity has never been established (Cobb, 1992; Grossmann, 2000). Intriguingly, a dominant negative mutation in an actin isoform induces cell death in trichoblasts (Nishimura *et al.*, 2003) and disrupting actin causes apoptosis in pollen tubes (Thomas *et al.*, 2006). If actin disruption is widely linked to apoptosis in higher plant cells, then this might explain the toxicity of 2,4-D.

The role of actin in the mechanism of auxin-induced root growth inhibition

That compounds depleting actin concomitantly decrease cell production is consistent with the known involvement of actin with the phragmoplast and preprophase band (Ingouff *et al.*, 2005; Mineyuki, 1999; Sano *et al.*, 2005; Smith, 1999). Likewise, aberrant cell division occurs in the roots of an *Arabidopsis* mutant, *act7-4*, that contains low levels of ACT7, an abundant actin isoform in the root growth zone (Gilliland *et al.*, 2003). In the rice coleoptile, IAA-stimulated cell growth has been argued to be related to the formation of fine networks of actin (Holweg *et al.*, 2004; Wang and Nick, 1998), and it could be that the tendency to increased actin bundling, seen here for IAA, NAA and TIBA, reflects the loss of such networks. However, for the root, IAA (and the related

compounds) reduced the size of the elongation zone rather than the process of cellular expansion.

The compounds disrupting actin failed to reduce maximal elemental elongation rate appreciably; not at all for 2,4-D and by 20% for NPA (data not shown) and 25% for latrunculin (Tables 2 and 3). This is surprising because all plant cell growth is assumed to require actin. This assumption is well-established for tip growth, as well as for trichomes and the lobes of leaf epidermal cells (Hepler *et al.*, 2001; Smith and Oppenheimer, 2005); however, a requirement for actin in the specific process of diffuse expansion remains unclear.

Growth is altered when the actin cytoskeleton is disrupted genetically (Ramachandran *et al.*, 2000; Dong *et al.*, 2001; Kandasamy *et al.*, 2001; Ketelaar *et al.*, 2004) or by week-long inhibitor treatment (Baluška *et al.*, 2001); nevertheless, in such studies, growth was usually analyzed insufficiently to distinguish an altered intensity of the elongation process from an altered spatial or temporal span. What's more, in a mutant, secondary effects may occur. For example, Nishimura *et al.* (2003) reported that a dominant mutation in the ACT2 isoform of actin reduces root elongation; however, the mutation also causes cell death in trichoblasts, which could be responsible for the decreased root elongation. Therefore, while observations on mutants and transgenics have established a general role for actin in plant development, they do not contradict our finding for roots that the intensity of diffuse growth (i.e. elemental elongation rate) has a limited requirement for functional actin.

In stem or coleoptile segments, elongation is slowed by actin inhibitors (Cande *et al.*, 1973; Thimann *et al.*, 1992), which presumably reflects lower elongation intensity because the segments have little if any cell division and elongate more or less evenly over their lengths. However, actin inhibitors are relatively more effective against growth in stems than roots (Pope *et al.*, 1979). Whereas a cell in a stem elongates slowly (approximately 5% per hour) for several days, a cell in a root elongates rapidly (approximately 50% per hour) for several hours. We suggest that the system powering the slow but steady expansion of stem cells requires a functional actin cytoskeleton to a greater extent than does the explosive expansion of root cells.

Polar auxin-transport inhibitors and their interaction with actin

For decades, TIBA and NPA have been used to inhibit polar auxin transport, although the mechanism by which they act is unknown (Rubery, 1987; Bennett *et al.*, 1998). Interestingly, we found that NPA and TIBA affect actin organization differently (Figure 7). While TIBA seemed to bundle actin, NPA disrupted actin. In cultured tobacco cells, NPA did not affect actin (Petrásek *et al.*, 2003); the difference between the *Arabidopsis* root and the tobacco cells requires elucidation.

In theory, TIBA and NPA should mimic the effect of IAA on actin, insofar as the intracellular concentration of auxin in the root increases when polar transport is blocked (Ljung *et al.*, 2005). This prediction appears to be met for TIBA as well as for the *eir1* mutant (Figure 7 and Tables 1 and 4) but not for NPA. Actin-based motility might be required for polar auxin transport, but the unaffected gravitropism in roots treated for 2 days with 30 nM 2,4-D or 17 nM latrunculin (data not shown) argues against this, as does the fact that cytochalasin B has no effect on the rate of polar transport (although delaying uptake) in stems or coleoptiles at a concentration that stops cytoplasmic streaming (Cande *et al.*, 1973). NPA might affect actin directly, based on studies that find NPA-binding activity associated with actin fractions (Butler *et al.*, 1998; Cox and Muday, 1994; Hu *et al.*, 2000). It would be interesting to determine whether similar fractions bind 2,4-D.

The role of actin in targeting the auxin efflux proteins, PIN1 and PIN2

Auxin is moved throughout the whole plant by plasma membrane proteins, including the PIN family, which are involved with efflux (Blakeslee *et al.*, 2005; Petrásek *et al.*, 2006). PIN proteins cycle dynamically between plasma membrane and endosomes (Murphy *et al.*, 2005). The cycling has been hypothesized to depend on actin, based on the ability of cytochalasin to prevent the mislocalization of PIN1 caused by brefeldin A (Geldner *et al.*, 2001). Here, we find that, for both long-term (2 days, Figure 9) and short-term (2 h, Figure 10) treatments, PIN localization did not suffer in the presence of latrunculin, cytochalasin (not shown), NPA or 2,4-D at concentrations where actin function was disrupted enough to slow cytoplasmic streaming and cell division. Treatment with latrunculin caused PIN2 to accumulate in bodies of unknown identity; however, this occurred only in the epidermis with two-day treatment, to a much lesser extent with cytochalasin, and did not prevent polar PIN2 targeting. Although some actin remained in the latrunculin, 2,4-D and NPA treatments, such remnants are the least likely to support the kind of dynamic motility considered to drive PIN cycling.

Observations indicating a role for actin in targeting PIN1 have involved combined treatments with an actin inhibitor and brefeldin; treatments with an actin inhibitor alone seldom alter the subcellular localization of PIN1 (Boutte *et al.*, 2006; Friml *et al.*, 2002; Geldner *et al.*, 2001; Kleine-Vehn *et al.*, 2006). In these reports, stable localization could reflect interruption by the actin inhibitors of flow to, as well as from, the plasma membrane; but, over a two-day treatment, PINs would be expected to become delocalized by diffusion, or to be aberrant in the cells produced during the 2 days (>60 cells per cortical file; Table 1). Furthermore, short-term treatment with cytochalasin caused rapid inter-

nalization of PIN3, a protein expressed in root cap and re-localized rapidly during gravitropism (Friml *et al.*, 2002). Therefore, the evidence to date, while consistent with an actin-based deployment mechanism for PIN3, is most simply interpreted as showing that PIN1 and PIN2 are targeted by an actin-independent mechanism.

Experimental procedures

Plant material, growth conditions and chemicals

All lines are in the Columbia background of *Arabidopsis thaliana* (L.) Heynh. The transgenic ABD2-GFP line has been described previously by Wang *et al.* (2004), and the PIN2-GFP line, described by Xu and Scheres (2005b), was the gift of B. Scheres (University of Utrecht, The Netherlands). The *eir1-1* and *aux-1-7* mutations were introduced into the ABD2-GFP line by crossing, and independent lines homozygous for the mutation and expressing the reporter were identified by screening for fluorescence and an agravitropic phenotype. Surface-sterilized seeds were placed in round, 10 cm Petri plates on modified Hoagland's medium (Baskin and Wilson, 1997), 1% w/v sucrose and 1% w/v agar (Difco Bacto agar, BD Laboratories; <http://www.bd.com>). For latrunculin B treatment, 6 cm diameter Petri plates were used. Two days after stratification at 4°C in the dark, plates were transferred to a growth chamber at 23°C under continuous yellow light at an intensity of 100–120 $\mu\text{mol m}^{-2} \text{sec}^{-1}$. NPA was purchased from Pfaltz and Bauer (<http://www.pfaltzandbauer.com/>).

Growth, cell length and cell production rate assays

Seedlings were grown vertically for 4 days after stratification. On day 4, seedlings were transferred to medium with or without supplementation and grown vertically for another 2–3 days. All auxins and inhibitors were dissolved initially in DMSO and diluted into molten agar just prior to gelling. The dilution was 1000-fold and control media received an equivalent volume of DMSO. For the short-term assay, 4-day-old seedlings were placed on liquid Hoagland's medium supplemented with or without growth regulators and incubated for 2 h.

Root elongation rate was measured by scoring the position of the root tip on the back of the Petri plate once per day, as described by Baskin and Wilson (1997). Cortical cell length was measured using Nomarski optics and a 20 x, 0.5 NA objective. To ensure newly matured cells were scored, no cell was measured closer to the tip than the position where root hair length was roughly half maximal. The length of 20 mature cortical cells was measured from each root, with eight roots used per treatment. Cell production rate was calculated by taking the ratio of root elongation rate and average cell length for each individual and averaging over all the roots in the treatment. The reported experiments are based on three replicates per treatment; all of these experiments have themselves been repeated several times.

Imaging and spatial analysis of elongation were performed as described previously (van der Weele *et al.*, 2003) with minor modifications. Briefly, a Petri plate was placed on the stand of a horizontal microscope and the root imaged with a 10x lens through the agar. An image sequence of nine images was obtained at 15 sec intervals, the stage was translocated to an adjacent region of the growth zone and another sequence was obtained, continuing for four to eight sequences until the growth zone was spanned.

A complete velocity profile was then calculated automatically by RootflowRT software (available from http://meru.rnet.missouri.edu/mvl/bio_motion/). To analyze the velocity profiles, a novel logistic function was fitted to the data using a non-linear curve fitting routine (Sigma Plot version 7; SPSS, <http://www.spss.com/>). The function and its applicability to high-resolution velocity profiles have been described elsewhere (Peters and Baskin, 2006). For experiments, a Petri plate was brought from the growth chamber to the microscope, the image sequences obtained, and the plate returned to the growth chamber. On a given day, three to five roots each for several treatments were imaged, always including controls. Parameters reported are pooled from between six and 12 roots imaged on at least three different days.

GUS staining and immunostaining

GUS staining was performed on transgenic seedlings expressing a cyclinB1;1-GUS reporter construct (Colón-Carmona *et al.*, 1999). Three-day-old seedlings were transferred to Murashige and Skoog plates supplemented with auxins as indicated. After 48 h, 10–15 seedlings from each treatment were processed to image GUS expression by incubating seedlings in staining solution (100 mM sodium phosphate buffer, pH 7.0, 10 mM EDTA, 0.5 mM potassium ferricyanide, 0.5 mM potassium ferrocyanide, 0.5% Triton X-100 and 2 mM X-glucuronide) at 37°C for 3 h. Seedlings were washed three times with 100 mM sodium phosphate buffer (pH 7.0), and roots were examined through a compound microscope and photographed with a color digital camera.

To localize actin, we used the protocol described by Bannigan *et al.* (2006) with minor modifications. Briefly, roots were fixed in PIPES buffer containing paraformaldehyde, glutaraldehyde and calcium, permeabilized in Triton and cold methanol, successively, and subjected to brief cell-wall digestion with pectinase and pectolyase. The modifications include the addition of 400 µM maleimidobenzoyl-*N*-hydroxy succinimide (MBS) to the fixation buffer, extracting with Triton X-100 before cell-wall digestion, rather than after, and at a concentration of 1% v/v, and the use of a mouse monoclonal anti-(chicken gizzard) actin (C4; Chemicon, <http://www.chemicon.com/>), diluted 1:1000 in PBS, 1% BSA and 0.01% sodium azide (PBA).

To localize PINs, the protocol described above was used, except that glutaraldehyde and MBS were omitted, and, after the cold methanol treatment and rehydration in PBS, seedlings were incubated in 10% v/v DMSO and 3% v/v NP-40 in PME [50mM PIPES pH7, 2mM MgSO₄ and 5mM EGTA (PME)] for 1 h. After incubation, seedlings were rinsed PME (3 × 5 min) and blocked in 1% w/v goat serum in PBA, and after 1 h, the blocking solution was replaced carefully with primary antibody. The primary antibodies were anti-PIN2 (1:100 dilution), the gift of P. Masson (University of Wisconsin, Madison, USA) or anti-PIN1 (1:100 dilution), the gift of J. Friml (University of Tübingen, Germany). The secondary antibody was Cy-3 goat anti-rabbit IgG (1:200, Jackson Immunoresearch, <http://www.jacksonimmuno.com/>). All imaging was done on a confocal fluorescence microscope (LSM 510 Meta; Carl Zeiss; <http://www.zeiss.com/>) equipped with a 63× oil-immersion objective. Individual stacks or projections were assembled using Zeiss software.

Quantifying the extent of actin polymerization

Actin polymerization was quantified using an image-processing routine developed previously (Tian *et al.*, 2004). Briefly, images were thresholded, skeletonized, and the area of the skeleton recorded as a

percentage of the sampled area. Skeletonizing sharply reduces the dependence of the area on the choice of threshold. Images used were of the elongation zone (as in Figure 5, upper row), and the sampled area comprised all (or most) of the root in the image. Images were excluded that had prominent central vacuoles or high cytoplasmic background. The data set (Figure 8) reflects a majority of the elongation zone images collected over the roughly two years of this study.

Acknowledgements

This work was supported in part by the US Department of Energy (award 03ER15421 to T.I.B.), which does not constitute endorsement by that department of views expressed herein, by the US National Institutes of Health (award EB00573-01A1 to K. Palaniappan, University of Missouri-Columbia), and by the US National Science Foundation (awards IBN 0316876 to T.I.B., and DBI-0400580 to E.B.). The confocal microscopy was accomplished at the Central Microscopy Facility at the University of Massachusetts, Amherst, USA. We thank Patrick Masson (University of Wisconsin, USA) for anti-PIN2, Jiri Friml (University of Tübingen, Germany) for anti-PIN1 and Ben Scheres (University of Utrecht, The Netherlands) for the GFP-PIN2 line. We acknowledge insightful help with curve fitting from Winfried Peters (Purdue University, Fort Wayne, Indiana, USA), and thank our colleagues Peter K. Hepler and Magdalena Bezanilla for judicious comments on the manuscript.

Supplementary material

The following supplementary material is available for this article online:

Movies S1–S4. The effects of compounds on cytoplasmic streaming in root epidermal cells.

Figure S1. Effects of auxins and other compounds on the localization of PIN1.

This material is available as part of the online article from <http://www.blackwell-synergy.com>

References

- Badescu, G.O. and Napier, R.M.** (2006) Receptors for auxin: will it all end in TIRs? *Trends Plant Sci.* **11**, 217–223.
- Baluška, F., Jasik, J., Edelmann, H.G., Salajova, T. and Volkmann, D.** (2001) Latrunculin B-induced plant dwarfism: plant cell elongation is F-actin-dependent. *Dev. Biol.* **231**, 113–124.
- Bannigan, A., Wiedemeier, A.M., Williamson, R.E., Overall, R.L. and Baskin, T.I.** (2006) Cortical microtubule arrays lose uniform alignment between cells and are oryzalin resistant in the arabidopsis mutant *radially swollen 6*. *Plant Cell Physiol* **47**, 949–958.
- Baskin, T.I. and Wilson, J.E.** (1997) Inhibitors of protein kinases and phosphatases alter root morphology and disorganize cortical microtubules. *Plant Physiol.* **113**, 493–502.
- Beemster, G.T.S. and Baskin, T.I.** (1998) Analysis of cell division and elongation underlying the developmental acceleration of root growth in *Arabidopsis thaliana*. *Plant Physiol.* **116**, 1515–1526.
- Beemster, G.T.S. and Baskin, T.I.** (2000) STUNTED PLANT1 mediates effects of cytokinin, but not of auxin, on cell division and expansion in the root of *Arabidopsis*. *Plant Physiol.* **124**, 1718–1727.
- Beemster, G.T.S., De Vusser, K., De Tavernier, E., De Bock, K. and Inzé, D.** (2002) Variation in growth rate between *Arabidopsis*

- ecotypes is correlated with cell division and A-type cyclin-dependent kinase activity. *Plant Physiol.* **129**, 854–864.
- Bennett, M.J., Marchant, A., May, S.T. and Swarup, R.** (1998) Going the distance with auxin: unravelling the molecular basis of auxin transport. *Philos. Trans. R. Soc. Lond. [Biol.]* **353**, 1511–1515.
- Blakeslee, J.J., Peer, W.A. and Murphy, A.S.** (2005) Auxin transport. *Curr. Opin. Plant Biol.* **8**, 494–500.
- Boonsirichai, K., Sedbrook, J.C., Chen, R., Gilroy, S. and Masson, P.H.** (2003) ALTERED RESPONSE TO GRAVITY is a peripheral membrane protein that modulates gravity-induced cytoplasmic alkalization and lateral auxin transport in plant statocytes. *Plant Cell*, **15**, 2612–2625.
- Boutte, Y., Crosnier, M.T., Carraro, N., Traas, J. and Satiat-Jeunemaitre, B.** (2006) The plasma membrane recycling pathway and cell polarity in plants: studies on PIN proteins. *J. Cell Sci.* **119**, 1255–1265.
- Butler, J.H., Hu, S., Brady, S.R., Dixon, M.W. and Muday, G.K.** (1998) *In vitro* and *in vivo* evidence for actin association of the naphthylphthalamic acid-binding protein from zucchini hypocotyls. *Plant J.* **13**, 291–301.
- Campanoni, P. and Nick, P.** (2005) Auxin-dependent cell division and cell elongation. 1-naphthaleneacetic acid and 2,4-dichlorophenoxyacetic acid activate different pathways. *Plant Physiol.* **137**, 939–948.
- Cande, W.Z., Goldsmith, M.H.M. and Ray, P.M.** (1973) Polar auxin transport and auxin-induced elongation in the absence of cytoplasmic streaming. *Planta*, **111**, 279–296.
- Chen, J.G.** (2001) Dual auxin signalling pathways control cell elongation and division. *J. Plant Growth Regul.* **20**, 255–264.
- Cobb, A.H.** (1992) Auxin-type herbicides. In *Herbicides and Plant Physiology* (Cobb, A.H., ed.). London: Chapman and Hall, pp. 82–106.
- Colón-Carmona, A., You, R., Haimovitch-Gal, T. and Doerner, P.** (1999) Spatio-temporal analysis of mitotic activity with a labile cyclin-GUS fusion protein. *Plant J.* **20**, 503–508.
- Cox, D.N. and Muday, G.K.** (1994) NPA binding activity is peripheral to the plasma membrane and is associated with the cytoskeleton. *Plant Cell*, **6**, 1941–1953.
- Davies, P.J., Doró, J.A. and Tarbox, A.W.** (1976) The movement and physiological effect of indoleacetic acid following point applications to root tips of *Zea mays*. *Physiol. Plant.* **36**, 333–337.
- Dong, C.H., Xia, G.X., Hong, Y., Ramachandran, S., Kost, B. and Chua, N.H.** (2001) ADF proteins are involved in the control of flowering and regulate F-actin organization, cell expansion, and organ growth in Arabidopsis. *Plant Cell*, **13**, 1333–1346.
- Friml, J., Wiśniewska, J., Benková, E., Mendgen, K. and Palme, K.** (2002) Lateral relocation of auxin efflux regulator PIN3 mediates tropism in Arabidopsis. *Nature*, **415**, 806–809.
- Geldner, N., Friml, J., Stierhof, Y.D., Jürgens, G. and Palme, K.** (2001) Auxin transport inhibitors block PIN1 cycling and vesicle trafficking. *Nature*, **413**, 425–428.
- Gilliland, L.U., Pawloski, L.C., Kandasamy, M.K. and Meagher, R.B.** (2003) Arabidopsis actin gene *ACT7* plays an essential role in germination and root growth. *Plant J.* **33**, 319–328.
- Goodwin, R.H.** (1972) Studies on roots: V. Effects of indoleacetic acid on the standard root growth pattern of *Phleum pratense*. *Bot. Gaz.* **133**, 224–229.
- Green, P.B.** (1976) Growth and cell pattern formation on an axis: critique of concepts, terminology and modes of study. *Bot. Gaz.* **137**, 187–202.
- Grossmann, K.** (2000) Mode of action of auxin herbicides: a new ending to a long, drawn out story. *Trends Plant Sci.* **5**, 506–508.
- Hejnowicz, Z.** (1961) The response of the different parts of the cell elongation zone in root to external β -indolylacetic acid. *Acta Soc. Bot. Polon.* **30**, 25–42.
- Hepler, P.K., Vidali, L. and Cheung, A.Y.** (2001) Polarized cell growth in higher plants. *Annu. Rev. Cell Dev. Biol.* **17**, 159–187.
- Holweg, C., Suslin, C. and Nick, P.** (2004) Capturing *in vivo* dynamics of the actin cytoskeleton stimulated by auxin or light. *Plant Cell Physiol.* **45**, 855–863.
- Hu, S., Brady, S.R., Kovar, D.R., Staiger, C.J., Clark, G.B., Roux, S.J. and Muday, G.K.** (2000) Identification of plant actin-binding proteins by F-actin affinity chromatography. *Plant J.* **24**, 127–137.
- Ingouff, M., Gerald, J.N.F., Guerin, C., Robert, H., Sorensen, M.B., Van Damme, D., Geelen, D., Blanchoin, L. and Berger, F.** (2005) Plant formin AtFH5 is an evolutionarily conserved actin nucleator involved in cytokinesis. *Nat. Cell Biol.* **7**, 374–380.
- Kandasamy, M.K., Gilliland, L.U., McKinney, E.C. and Meagher, R.B.** (2001) One plant actin isoform, ACT7, is induced by auxin and required for normal callus formation. *Plant Cell*, **13**, 1541–1554.
- Kepinski, S. and Leyser, O.** (2005) The Arabidopsis F-box protein TIR1 is an auxin receptor. *Nature*, **435**, 446–451.
- Ketelaar, T., Allwood, E.G., Anthony, R., Voigt, B., Menzel, D. and Hussey, P.J.** (2004) The actin-interacting protein AIP1 is essential for actin organization and plant development. *Curr. Biol.* **14**, 145–149.
- Kleine-Vehn, J., Dhonukshe, P., Swarup, R., Bennett, M. and Friml, J.** (2006) Subcellular trafficking of the Arabidopsis auxin influx carrier AUX1 uses a novel pathway distinct from PIN1. *Plant Cell*, **18**, 3171.
- Liszskay, A., van der Zalm, E. and Schopfer, P.** (2004) Production of reactive oxygen intermediates ($O_2^{\cdot-}$, H_2O_2 , and $\cdot OH$) by maize roots and their role in wall loosening and elongation growth. *Plant Physiol.* **136**, 3114–3123.
- Ljung, K., Hull, A.K., Celenza, J., Yamada, M., Estelle, M., Normanly, J. and Sandberg, G.** (2005) Sites and regulation of auxin biosynthesis in Arabidopsis roots. *Plant Cell*, **17**, 1090–1104.
- Lovy-Wheeler, A., Wilsen, K.L., Baskin, T.I. and Hepler, P.K.** (2005) Enhanced fixation reveals the apical cortical fringe of actin filaments as a consistent feature of the pollen tube. *Planta*, **221**, 95–104.
- Luschnig, C., Gaxiola, R.A., Grisafi, P. and Fink, G.R.** (1998) EIR1, a root-specific protein involved in auxin transport, is required for gravitropism in *Arabidopsis thaliana*. *Genes Dev.* **12**, 2175–2187.
- Meuwly, P. and Pilet, P.-E.** (1991) Local treatment with indole-3-acetic acid induces differential growth responses in *Zea mays* L. roots. *Planta*, **185**, 58–64.
- Mineyuki, Y.** (1999) The preprophase band of microtubules: its function as a cytokinetic apparatus in higher plants. *Int. Rev. Cytol.* **187**, 1–49.
- Muday, G.K. and Murphy, A.S.** (2002) An emerging model of auxin transport regulation. *Plant Cell*, **14**, 293–299.
- Murphy, A.S., Bandyopadhyay, A., Holstein, S.E. and Peer, W.A.** (2005) Endocytotic cycling of PM proteins. *Annu. Rev. Plant Biol.* **56**, 221–251.
- Nishimura, T., Yokota, E., Wada, T., Shimmen, T. and Okada, K.** (2003) An Arabidopsis *ACT2* dominant-negative mutation, which disturbs F-actin polymerization, reveals its distinctive function in root development. *Plant Cell Physiol.* **44**, 1131–1140.
- Peters, W.S. and Baskin, T.I.** (2006) Tailor-made composite functions as tools in model choice: the case of sigmoidal versus bi-linear growth profiles. *Plant Methods*, **2**, 12.
- Petrásek, J., Cerna, A., Schwarzerova, K., Elckner, M., Morris, D.A. and Zazimalova, E.** (2003) Do phytoalexins inhibit auxin efflux by impairing vesicle traffic? *Plant Physiol.* **131**, 254–263.

- Petrásek, J., Mravec, J., Bouchard, R. et al.** (2006) PIN proteins perform a rate-limiting function in cellular auxin efflux. *Science*, **312**, 914–918.
- Pope, D.G., Thorpe, J.R., Al-Azzawi, M.J. and Hall, J.L.** (1979) The effect of cytochalasin B on the rate of growth and ultrastructure of wheat coleoptiles and maize roots. *Planta*, **144**, 373–383.
- Rahman, A., Ahamed, A., Amakawa, T., Goto, N. and Tsurumi, S.** (2001) Chromosaponin I specifically interacts with AUX1 protein in regulating the gravitropic response of Arabidopsis roots. *Plant Physiol.* **125**, 990–1000.
- Rahman, A., Nakasone, A., Chhun, T., Ooura, C., Biswas, K.K., Uchimiya, H., Tsurumi, S., Baskin, T.I., Tanaka, A. and Oono, Y.** (2006) A novel protein, SMAP1, mediates responses of the Arabidopsis root to the synthetic auxin 2,4-dichlorophenoxyacetic acid. *Plant J.* **47**, 788–801.
- Ramachandran, S., Christensen, H.E., Ishimaru, Y., Dong, C.H., Chao-Ming, W., Cleary, A.L. and Chua, N.H.** (2000) Profilin plays a role in cell elongation, cell shape maintenance, and flowering in Arabidopsis. *Plant Physiol.* **124**, 1637–1647.
- Rashotte, A.M., Poupard, J., Waddell, C.S. and Muday, G.K.** (2003) Transport of the two natural auxins, indole-3-butyric acid and indole-3-acetic acid, in Arabidopsis. *Plant Physiol.* **133**, 761–772.
- Rubery, P.H.** (1987) Auxin Transport. In *Plant Hormones and Their Role in Plant Growth and Development* (Davies, P.J., ed.). Dordrecht, The Netherlands: Martinus Nijhoff, pp. 341–362.
- Sano, T., Higaki, T., Oda, Y., Hayashi, T. and Hasezawa, S.** (2005) Appearance of actin microfilament 'twin peaks' in mitosis and their function in cell plate formation, as visualized in tobacco BY-2 cells expressing GFP-fimbrin. *Plant J.* **44**, 595–605.
- Silk, W.K.** (1992) Steady form from changing cells. *Int. J. Plant Sci.* **153**, S49–S58.
- Silk, W.K., Lord, E.M. and Eckard, K.J.** (1989) Growth patterns inferred from anatomical records. Empirical tests using longisections of roots of *Zea mays* L. *Plant Physiol.* **90**, 708–713.
- Smith, L.G.** (1999) Divide and conquer: cytokinesis in plant cells. *Curr. Opin. Plant Biol.* **2**, 447–453.
- Smith, L.G. and Oppenheimer, D.G.** (2005) Spatial control of cell expansion by the plant cytoskeleton. *Annu. Rev. Cell Dev. Biol.* **21**, 271–295.
- Stasinopoulos, T.C. and Hangarter, R.P.** (1990) Preventing photochemistry in culture media by long-pass filters alters growth of cultured tissues. *Plant Physiol.* **93**, 1365–1369.
- Sweeney, B.M. and Thimann, K.V.** (1938) The effect of auxins on protoplasmic streaming. II. *J. Gen. Physiol.* **21**, 439–461.
- Taiz, L. and Zeiger, E.** (2006) Auxin: The growth hormone. In *Plant Physiology*, 4th edn. Sunderland, MA: Sinauer Associates, pp. 468–507.
- Thimann, K.V., Reese, K. and Nachmias, V.T.** (1992) Actin and the elongation of plant cells. *Protoplasma*, **171**, 153–166.
- Thomas, S.G., Huang, S.J., Li, S.T., Staiger, C.J. and Franklin-Tong, V.E.** (2006) Actin depolymerization is sufficient to induce programmed cell death in self-incompatible pollen. *J. Cell Biol.* **174**, 221–229.
- Tian, G.W., Smith, D., Glück, S. and Baskin, T.I.** (2004) The higher plant cortical microtubule array analyzed *in vitro* in the presence of the cell wall. *Cell Motil. Cytoskel.* **57**, 26–36.
- Ullah, H., Chen, J.-G., Temple, B., Boyes, D.C., Alonso, J.M., Davis, K.R., Ecker, J.R. and Jones, A.M.** (2003) The β -subunit of the Arabidopsis G-protein negatively regulates auxin-induced cell division and affects multiple developmental processes. *Plant Cell*, **15**, 393–409.
- Vidali, L., McKenna, S.T. and Hepler, P.K.** (2001) Actin polymerization is essential for pollen tube growth. *Mol. Biol. Cell.* **12**, 2534–2545.
- Wang, Q.Y. and Nick, P.** (1998) The auxin response of actin is altered in the rice mutant Yin-Yang. *Protoplasma*, **204**, 22–33.
- Wang, Y.S., Motes, C.M., Mohamalwari, D.R. and Blancaflor, E.B.** (2004) Green fluorescent protein fusions to Arabidopsis fimbrin 1 for spatio-temporal imaging of F-actin dynamics in roots. *Cell Motil. Cytoskel.* **59**, 79–93.
- van der Weele, C.M., Jiang, H.S., Palaniappan, K.K., Ivanov, V.B., Palaniappan, K. and Baskin, T.I.** (2003) A new algorithm for computational image analysis of deformable motion at high spatial and temporal resolution applied to root growth. Roughly uniform elongation in the meristem and also, after an abrupt acceleration, in the elongation zone. *Plant Physiol.* **132**, 1138–1148.
- Williamson, R.E.** (1993) Organelle movements. *Annu. Rev. Plant Physiol. Plant Mol. Biol.* **44**, 181–202.
- Woodward, A.W. and Bartel, B.** (2005) Auxin: regulation, action, and interaction. *Ann. Bot.* **95**, 707–735.
- Xu, J. and Scheres, B.** (2005a) Cell polarity: ROPing the ends together. *Curr. Opin. Plant Biol.* **8**, 613–618.
- Xu, J. and Scheres, B.** (2005b) Dissection of Arabidopsis ADP-RIBOSYLATION FACTOR 1 function in epidermal cell polarity. *Plant Cell*, **17**, 525–536.
- Yang, Z.** (2002) Small GTPases: versatile signaling switches in plants. *Plant Cell*, **14S**, 159–187.